Final published article:
Girmay, N., Miranda, E. and Poulos, A., 2024. Orientation and intensity of maximum response spectral ordinates during the December 20, 2022 Mw 6.4 Ferndale, California earthquake. *Soil Dynamics and Earthquake Engineering*, 176, p.108323.
https://doi.org/10.1016/j.soildyn.2023.108323

Orientation and intensity of maximum response spectral ordinates during the December 20, 2022 M_w 6.4 Ferndale, California earthquake

Nathan Girmay[1*], Eduardo Miranda[1], Alan Poulos[1]

[1]Department of Civil and Environmental Engineering, Stanford University, Stanford, California, U.S.A

* Corresponding author. *Email:* ngirmay3@stanford.edu

Highlights

- Orientation of the maximum response occurred close to the transverse orientation.
- This is consistent with recent observations from other strike-slip earthquakes.
- Spectral response at transverse orientation, on average, was close to RotD100.
- This was observed for oscillators with periods ranging from 0.1 s to 10 s.

Keywords

Ground motion directionality; Transverse orientation; Ground motion polarization; Response spectral ordinates; Ground motion intensity.

Abstract

The level of horizontal ground motion intensity can have large variations from one orientation to another. This study examines the orientation of the maximum response of 5%-damped linear oscillators and its geographical distribution for ground motions recorded during the December 20, 2022, Ferndale, CA earthquake. The orientation of the maximum intensity is found to generally occur close to the transverse orientation for epicentral distances greater than 30 km. At epicentral distances less than 30 km, the angular difference between the orientation of the maximum intensity and transverse orientation does not show a clear predominant orientation. The angular difference with respect to the transverse orientation is found to be strongly correlated with the level of intensity. The ground motion intensity at the transverse orientation was, on average, between 85% to 95% of the maximum intensity and was 1.0 to 1.26 times greater than the RotD50 intensity (i.e., the median intensity from all horizontal orientations). The level of polarization increases with the period of the oscillation and ground motions remain fairly polarized up to 350 km from the epicenter. The results support a case for future incorporation of directionality effects, and in particular, the use of orientation relative to the transverse orientation, when estimating response spectral ordinates from strike-slip earthquakes.

1. Introduction

In earthquake-resistant design, the most common measure of ground motion intensity is the 5%-damped response spectral ordinate, which represents the peak response of a single-degree-of-freedom linear-elastic oscillator with 5% damping subjected to a given ground motion. It has long been known that horizontal ground motion intensity, including the commonly used 5%-damped response spectral ordinate, varies with changes in orientation (i.e., changes in the azimuth considered at the given station) in what is referred to as directionality. Although horizontal earthquake ground motion intensity, in general, is recorded in two perpendicular orientations and exhibits different amplitudes in different horizontal orientations, only a single measure of ground motion intensity is typically used in current ground motion models (GMMs), essentially ignoring directionality effects. There have been several approaches for obtaining a single measure of intensity to represent the horizontal ground motion intensity that occurred at a site. The four most common methods that have been used in the past are: (1) combining the two as-recorded horizontal intensities such as by using their geometric mean (e.g., Joyner and Boore, 1982; Boore et al., 1997; Abrahamson and Silva, 1997; Beyer and Bommer, 2006); (2) selecting one of the two as-recorded horizontal intensities, what has typically been referred to as the arbitrary component (e.g., Boore et al., 1997); (3) using a horizontal intensity that is independent of the orientation of horizontal sensors (e.g., Boore et al., 2006; Boore et al., 2010); and (4) selecting the intensity occurring at a specific orientation with respect to the strike of the rupture such as strike-normal and strike-parallel components (e.g., Somerville et al., 1997).

Recent studies have shown that directionality effects can be significant. In other words, at a given site, the level of intensity can have large variations from one horizontal orientation to another (Hong and Goda, 2007; Shahi and Baker, 2014; Poulos and Miranda, 2022b). For example, using the NGA-West2 ground motion database, Poulos et al. (2022) found that 5%-damped response spectral ordinates at the maximum intensity are, on average, 1.3 to 2.0 times higher than the response spectral ordinate in the perpendicular direction depending on the period of the oscillator. However, for many years, directionality was not taken into account for design in the United States (U.S.) and it is still neglected in most countries. In the U.S., directionality was considered indirectly, starting with the 2010 version of ASCE 7, by using approximate amplification factors to estimate the intensity at the orientation of the maximum intensity (RotD100) from the median intensity from all orientations (RotD50). Since most GMMs do not use RotD100, ASCE 7 uses approximate period-dependent amplification factors to construct the design spectrum (ASCE, 2010; Poulos and Miranda, 2022a). Nonetheless, the factors used for the short-period response spectral region (0.2 s) in ASCE 7-10 underestimated the required amplification (Shahi and Baker, 2014). This has now been amended, with ASCE 7-22 incorporating improved period-dependent amplification factors at 22 different periods instead of only at 0.2 s and 1.0 s (ASCE, 2022).

Except for near-fault sites (i.e., source-to-site distances shorter than 5 to15 km), the orientation of the maximum intensity is currently considered to be uniformly distributed (Huang et al., 2008; NEHRP Consultants Joint Venture, 2011; Shahi and Baker, 2014). Accordingly, current seismic design standards in the U.S. emphasize the lack of predominant orientation in sites that are not near-fault (ASCE, 2010; ASCE, 2016; ASCE, 2022; PEER, 2017).

Whilst there have been several investigations on the directionality of response spectral ordinates, practically all of them have focused only on whether the orientation of the maximum response occurs at or close to the strike-normal orientation. In other words, they were studying if the orientation of the maximum intensity was approximately the same in all recording stations and how close to the strike normal it was. Recently, Poulos and Miranda (2023) investigated the orientation of the maximum intensity of ground motion records from shallow crustal earthquakes in the NGA-West2 database (Ancheta et al., 2014), studying them separately for each event for a total of 1,966 and 2,226 ground motions recorded in strike-slip and reverse faulting earthquakes, respectively. Using these recorded ground motions, they showed that for strike-slip events, the orientation of the maximum intensity tended to be relatively close to the transverse orientation (i.e., an orientation perpendicular to the line segment connecting the epicenter to the recording station). Furthermore, they showed that the tendency for the orientation of the maximum intensity to be closer to the transverse orientation increases with increasing period of the oscillator. This observation by Poulos and Miranda (2023) is important as it suggests that the orientation of the maximum response of future earthquakes can be estimated from the position of the epicenter relative to the site of interest, thus improving the ability to estimate ground motion intensity at different orientations.

The December 20th, 2022, M_w 6.4 Ferndale earthquake is a well-recorded event with a strike-slip faulting style (with a rake angle of 7º (USGS, 2022)) that provides an important opportunity to independently evaluate the observations by Poulos and Miranda (2023). It also provides an opportunity to evaluate the amplitude of response spectral ordinates in the transverse orientation relative to the RotD100 intensity (which is currently used by design standards in the U.S.) and the RotD50 intensity (which is commonly used in recent GMMs). This information could then be used in combination with recent probabilistic directionality models (Poulos and Miranda, 2022a; 2022b) for the development of correction factors to existing RotD50 GMM to then estimate levels of ground motion intensity at specific orientations.

This work examines the orientation of the maximum response for 5%-damped linear-elastic oscillators subjected to ground motions recorded in the December 20, 2022, Ferndale earthquake in northern California. Additionally, it examines several aspects of the directionality of ground motions recorded in this event that were not studied by Poulos and Miranda (2023). In particular, the following aspects are studied: (a) geographical distribution of the level of polarization of ground motions, which in this paper refers to the amount of directionality, and its variation with changes in the period of vibration for linear-elastic oscillators; (b) geographic distribution of the orientation of the maximum response spectral ordinate for linear-elastic oscillators with different periods of vibration and the effect of source-to-site distance on this orientation; (c) level of amplitude in response spectral ordinates in the transverse and radial orientations relative to the maximum intensity (RotD100); (d) level of amplitude in response spectral ordinates in the transverse and radial orientations relative to RotD50 intensities; (e) probability of exceeding RotD50 intensities in transverse and radial orientations.

2. Selected earthquake ground motions

In this paper, records from the 2022 M_w 6.4 Ferndale earthquake are used to study the directionality of horizontal ground motion. The earthquake occurred on December 20, 2022, at 10:34 (UTC) (2:34 pm local time), with an epicenter located close to the coast of northern California, approximately 15 km southwest of Ferndale and 30 km south of Eureka, California (USGS, 2022). Focal mechanism suggests strike-slip faulting (with a rake angle of 7°) on a steeply dipping fault that strikes west-southwest. The epicenter is in the most seismically active region in California due to the intersection of three tectonic plates (i.e., the Pacific Plate, the North American Plate, and the Juan de Fuca Plate) known as the Mendocino Triple Junction. At the intersection of the three plates is the crossing of the northern tip of the San Andreas Fault, the Mendocino Fracture Zone, and the Cascadia Subduction Zone (Temblor, 2022). This region experienced a sequence of overlapping earthquakes of M_w 6.2 and 5.7 almost a year before the 2022 earthquake. In the past century, there have been at least 40 other earthquakes with $M_w \geq 6$, including six with $M_w \geq 7$, within roughly 250 km of the 2022 earthquake (USGS, 2022). For a detailed description of the seismicity of this region of California, the reader is referred to Bakum (2000). The earthquake resulted in widely distributed power loss and damage to numerous buildings in Humboldt County, with over 30 residential and commercial buildings found structurally unsafe (Petri and Lin, 2022).

For this study, ground motion data, as processed by California Geological Survey (CGS)/California Strong Motion Instrumentation Program (CSMIP) and United States Geologic Survey/National Strong Motion Project (NSMP) was obtained from the Center for Engineering Strong Motion Data (CESMD). The data processing performed by CGS/CSMIP or USGS/NSMP includes instrument correction, baseline correction, and band-pass filtering using acausal filters (CESMD). Processed records (i.e., Volume 2) included in the study were selected according to the following criteria: (1) the record must be available in both horizontal components at a given station; (2) the orientation and polarity of the horizontal sensors at the recording station must be available; (3) the recording station must be a free-field station or acceptably represent free-field conditions; (4) the corner frequency of the low-cut (high-pass) filter at both horizontal components must be shorter than 0.08 Hz; and (5) at least one of the two recorded horizontal components must have a peak ground velocity (PGV) greater than or equal to 1 cm/s.

Since previous studies have found that polarization increases with period (e.g., Poulos and Miranda, 2022b; 2023), it is of interest to consider records that allow the reliable calculation of response spectral ordinates at relatively long periods. Therefore, the fourth criterion ensures that the records have maximum usable periods equal or longer than 10 s, making them suitable to study directionality for oscillators with periods up to 10 s (Boore, 2004). The minimum level of ground motion intensity in the fifth criterion was selected as an easy-to-use criterion to achieve a strong signal-to-noise ratio up to periods of 10 s, again to be able to carefully examine directionality for oscillators with periods up to 10 s. Based on the selection criteria outlined above, 70 ground motion records were found to be usable in this study for oscillators with natural periods ranging between 0.1 s and 8.0 s, whilst 55 ground motion records were found usable for oscillators with periods ranging between 8.0 s and 10 s.

3. Orientation of maximum ground motion intensity

For a given event, a linear-elastic oscillator within a horizontal plane can exhibit notable directionality and polarization (i.e., significantly larger response in certain orientations than in others). A simple way to visualize the response of an oscillator within a plane is to cross-plot the relative displacement of an oscillator when subjected to the two recorded horizontal components, resulting in a vectorial representation of displacement in the plane, in what is called a hodograph or particle motion trace. Figure 1 shows the relative displacement hodographs of 5% damped linear elastic oscillators having periods of vibration of 10 s and 5 s when subjected to ground motions recorded during the 2022 M_w 6.4 Ferndale earthquake. The figure also shows the spatial distribution of the stations considered. In this figure, each hodograph has been normalized by its maximum spectral response (RotD100), which corresponds to the point farthest away from the origin (i.e., resting point) of the hodograph. Hence, all hodographs in this figure are shown with the same peak amplitude in order to better appreciate the directionality at each recording station. From this figure, it is apparent that stations close to each other tend to have response orientations that are similar to each other. This observation is only partly evident for recording stations that are near the epicenter (see the closeups on the right-hand side of Figure 1) but generally becomes more apparent at stations located further from the epicenter. Nonetheless, the hodographs visually demonstrate that the oscillator response at most stations is fairly polarized for this event, even at distances far from the source, with clearly noticeable directions of predominant response. It is to be noted that directionality is not necessarily related to forward directivity in the near-source region. As identified by Boore and Akkar

(2003), the intensity in two orthogonal orientations at a given site can be notably different, suggesting ground motion can be highly polarized even at distances very far from the source.

There are several ways in which the level of polarization in horizontal ground motion can be quantified. One of those is by using the ratio in intensities between the transverse and radial orientations. Figure 2 shows histograms of the ratio between ground motion intensities, as measured by response spectral ordinates, in the transverse orientation, Sa_T, and the intensity in the radial orientation, Sa_R, for periods of 3, 5, 7, and 10 s. It can be seen that these ratios are typically larger than one, with mean values ranging from 1.68 to 2.54 depending on the period of vibration of the oscillator, and that these ratios for some records at certain periods can be larger than five. Figure 3 shows the influence of the period of vibration on the level of polarization as measured by the mean ratio between the ground motion intensity at the transverse orientation and the intensity at the radial orientation. From this figure, it is clear that the level of polarization, on average, tends to increase as the fundamental period of the oscillator gets longer. Also shown in Figure 3 is the interquartile range from which one may infer that for periods of vibration longer than 2 s, there is at least a 75% chance that the 5%-damped spectral ordinate will be larger in the transverse orientation than in the radial orientation.

Figure 4 shows the orientation of the maximum response at each recording station of 5% damped linear elastic oscillators for periods of 3, 5, 7, and 10 s. At each recording station, this orientation of the maximum response is indicated by short black lines. As done by Poulos and Miranda (2023), the angular difference between the orientation of the maximum intensity and the transverse orientation is defined as the variable $\alpha \in [-90°, 90°]$, where a positive value corresponds to counterclockwise orientations with respect to the transverse orientation. The absolute angular difference between the orientation of the maximum intensity and the transverse orientation is $|\alpha| \in [0°, 90°]$. Figure 4 depicts the values of $|\alpha|$ at each station by the color inside the small circles, with blue indicating values closer to 0° (i.e., closer to the transverse orientation) and red indicating values closer to 90° (i.e., closer to the radial orientation). Evidently, across the four periods, the large majority of recording stations are colored blue, suggesting that the predominant orientation of the maximum intensity is much closer to the transverse orientation than to the radial orientation.

Histograms of $|\alpha|$ for oscillators with periods of 3, 5, 7, and 10 s are shown in Figure 5. It is readily apparent that the probability distribution of $|\alpha|$ is noticeably skewed to low values of $|\alpha|$, with most of the records having values of $|\alpha|$ below 45°. Should the orientation of the maximum intensity with respect to the transverse orientation be equally likely in any orientation, the histograms would appear as uniform distributions, as indicated by the blue discontinuous line in each of these histograms, and have a mean $|\alpha|$ of 45°. However, the mean $|\alpha|$ for the four periods is significantly below 45°, indicating that the orientations of the maximum intensity for this event are, on average, relatively close to the transverse orientations, consistent with recent observations by Poulos and Miranda (2023) for strike-slip events in the NGA-West2 ground motion database. This observation is true for all periods and becomes more apparent as the period of the oscillator increases. Figure 6 shows the fraction of recording stations where the orientation of the maximum intensity falls within ±25° of the transverse orientation. According to previous studies by Poulos and Miranda (2022b), within this range of orientations, the spectral ordinate will be, on average, within 10% of the maximum spectral ordinate from all orientations (i.e., within 10% of the RotD100 intensity). Should the orientation of RotD100 be fully random, that is, equally likely to occur in any orientation, the expected fraction of recording stations that would be within ±25° would be only approximately 28% (50°/180°). However, as shown in this figure, for oscillators with a period of approximately 3 s, orientations of RotD100 occurred within ±25° of the transverse orientation in more than 50% of the recording stations. Moreover, at a period of 7.5 s, this fraction of recording stations with orientations of the maximum response being within 25° of the transverse orientation increases to approximately 80%, which is significantly above and nearly three times larger than the 28% that would occur if the orientation of the maximum response were to be fully random, suggesting that the orientation of the maximum intensity is not uniform and that it occurs at orientations close to the transverse orientation.

Figure 7 shows the relationship between $|\alpha|$ and the ratio of intensity at the transverse orientation to the maximum intensity at each recorded station for a 10 s oscillator. From the figure, it is apparent that the spectral ordinate in the transverse orientation relative to the RotD100 intensity is strongly correlated with $|\alpha|$, closely following the cosine curve. In particular, when α is within ±25° of the transverse direction, the spectral ordinate in the transverse orientation is within 10% of the RotD100 intensity, suggesting that this range of orientations close to the transverse orientation is the one that will experience the strongest intensities. This figure indicates that the value of $|\alpha|$ could be used as a relatively good estimator of the level of ground motion intensity (i.e., smaller alpha translates to a larger intensity and approaches RotD100 at transverse orientation, approximately following the cosine). More importantly, the figure suggests that the drop in intensity at the transverse orientation is not significant for a notable range of $|\alpha|$. The level of ground motion intensity at the transverse orientation is discussed in greater detail in the following section of this paper.

While the influence of source-to-site distance on the orientation of the maximum intensity has been investigated on numerous occasions, the focus of most investigations has been the orientation with respect to strike-normal orientation (e.g., Huang et al., 2008; Shahi and Baker, 2014). To get a better understanding of the influence of distance on the orientation of the maximum intensity with respect to the transverse orientation, angular distances between the transverse orientation and RotD100 were binned by epicentral distance. Figure 8 shows the influence of epicentral distance on the histograms of $|\alpha|$ for oscillator periods of 5, 7, and 10 s. Although the number of records in each bin is relatively small for epicentral distances less than 30 km, the figure suggests that, for this earthquake, within the near field, $|\alpha|$ is approximately uniformly distributed with mean $|\alpha|$ values closer to 45° across the three periods of vibration. These results suggest that the orientation of the maximum intensity for near-fault sites does not necessarily occur close to the transverse orientation, but that, at least for this earthquake, they do not appear to correspond to the strike-normal orientation either as identified by others. However, for epicentral distances greater than 30 km, the histograms are clearly skewed toward small values of $|\alpha|$ and mean values of $|\alpha|$ are significantly below 45°, indicating that for this event, the orientation of the maximum intensity is, on average, close to the transverse orientation, which is consistent with recent findings by Poulos and Miranda (2023) for strike-slip earthquakes.

4. Intensity at transverse and radial orientations

From the results presented in the previous section, it is clear that the maximum intensity is not equally likely to occur in all horizontal orientations. While the computed mean $|\alpha|$ values are notably smaller than 45°, they are not always exactly 0°. Therefore, it is of interest to investigate the ground motion intensity in the transverse and radial orientation at each recorded station with respect to both RotD100 and RotD50.

Herein, an evaluation of the intensity in the transverse and radial orientation with respect to RotD100 is performed by computing the intensity ratios $Sa_T/Sa_{RotD100}$ and $Sa_R/Sa_{RotD100}$. Since RotD100 is the maximum intensity within the horizontal plane, the maximum possible intensity at the transverse or radial orientations is the RotD100 intensity. Thus, both $Sa_T/Sa_{RotD100}$ and $Sa_R/Sa_{RotD100}$ can range between 0 and 1. Figure 9 shows histograms of the ratio between the ground motion intensity at the transverse or radial orientation and RotD100 computed from ratios at all recording stations for periods of 3, 5, 7, and 10 s. As seen in the figure, the probability distribution of $Sa_T/Sa_{RotD100}$ ratios is heavily skewed towards large values for all four periods, with most ratios being relatively close to 1, indicating that the intensity at the transverse orientation is not much lower than the maximum intensity. For example, the intensity at the transverse orientation for an oscillator with a fundamental period of 3 s is, on average, 91% of the maximum intensity. The average of $Sa_T/Sa_{RotD100}$ ratios increases to 95% of RotD100 at 10 s. This contrasts significantly with the intensity at the radial orientation where $Sa_R/Sa_{RotD100}$ ratios exhibit a much larger variability and have mean values close to 0.5, that is, with intensities in the radial orientation that are on average approximately half of the maximum intensity, highlighting the importance of ground motion directionality.

A better understanding of the influence of oscillator period on $Sa_T/Sa_{RotD100}$ and $Sa_R/Sa_{RotD100}$ can be gained by considering how the mean ratio for all stations varies with changes in the period of vibration of the oscillator. Figure 10 shows the mean ratio between the ground motion intensity at the transverse or radial orientations and the RotD100 intensity for $T \in [0.1\text{ s}, 10\text{ s}]$. In this figure, variable $\theta \in \{0°, 90°\}$ is defined as the angular distance between the transverse orientation and the orientation of interest (i.e., $Sa(\theta = 0°)$ corresponds to the intensity at the transverse orientation). It can be seen that, even for short periods, the intensity at the transverse orientation is above 80% of the RotD100 intensity. Furthermore, as the oscillator period increases, the mean intensity at the transverse orientation also tends to increase, and by 3 s the average intensity at the transverse orientation is above 90% of the RotD100 intensity. In contrast, the intensity at the radial orientation exhibits strong reductions as the period increases. These results indicate that the significant increase in polarization with increasing periods is due not so much to the increase in intensity in the transverse orientation but to the reduction in intensity in the radial orientation. In this figure, the shaded areas around the means indicate the interquartile range for each period. It is discernable that there is significantly less variability in the $Sa_T/Sa_{RotD100}$ ratio than in the $Sa_R/Sa_{RotD100}$ ratio, with the band around the mean for the transverse orientation getting narrower with increasing period. Results shown in Figures 9 and 10 have important practical implications as they indicate that prediction of the exact orientation of RotD100 is not required since, for a wide range of angles close to the transverse direction, there is an intensity which is relatively close to the maximum intensity. The mean $Sa_T/Sa_{RotD100}$ ratio for this earthquake can be roughly approximated as

$$\frac{Sa_T}{Sa_{RotD100}} = 0.85 + \frac{T}{85} \qquad (1)$$

where T is the period of vibration of the oscillator in seconds. A similar fit can be performed using a larger database of ground motions from strike-slip events to obtain a more generalized equation to estimate the mean $Sa_T/Sa_{RotD100}$ for linear elastic oscillators.

As discussed in the introduction, most current GMMs use a single scalar measure of intensity in the horizontal orientation. Currently, the most commonly used scalar as a measure of horizontal ground motion intensity in GMMs is RotD50, which, for a given period of vibration, corresponds to the median intensity from all non-redundant horizontal orientations. Figure 11 shows the fraction of recording stations where the intensity at the transverse or the radial orientation exceeded the RotD50 intensity for periods of vibration ranging from 0.1 to 10 s. Evidently, a larger fraction of stations had intensities exceeding RotD50 in the transverse orientation when compared to those in the radial orientation. For very short periods of vibration, the intensity in the transverse orientation exceeded RotD50 in slightly more than 50% of the recording stations, with a tendency for this fraction to increase as the period of vibration increases. For periods of vibrations above 4 s, over 80% of the recording stations had an intensity in the transverse orientation that exceeds the RotD50 intensity.

The extent by which RotD50 intensity is exceeded in the transverse and radial orientation can be better understood by considering the mean variation of Sa_T/Sa_{RotD50} and Sa_R/Sa_{RotD50} with changes in the period of vibration of the oscillator. Since the intensity at the transverse or radial orientation can take a maximum value of RotD100, and since the maximum possible value for RotD100/RotD50 is $\sqrt{2}$ (which occurs, for example, in a fully polarized record, that is, one in which all the motion occurs at a specific orientation), both Sa_T/Sa_{RotD50} and Sa_R/Sa_{RotD50} range between 0 and $\sqrt{2}$. Figure 12 shows the mean ratio between the ground motion intensity at the transverse or radial orientation and the RotD50 intensity for $T \in [0.1 \text{ s}, 10 \text{ s}]$. For oscillators with a short period of vibration between 0.1 s and 0.3 s, the intensity at the transverse and radial orientations is, on average, approximately equal to RotD50. However, as the oscillator period increases, the average intensity at the transverse orientation increases from 1.0 to 1.26 times the RotD50 intensity. In contrast, the radial orientation is characterized by a significant reduction in intensity relative to the RotD50 intensity with increasing period. Additionally, as previously observed for the intensities relative to RotD100, the ratio of the intensity at the transverse orientation to RotD50 has a variability much smaller than that of the Sa_R/Sa_{RotD50} ratios. The mean ratios shown in Figure 12 could be used as correction factors to RotD50 intensities estimated using existing GMMs to estimate the level of intensity in the transverse orientation. However, it is unlikely for a given structure to have primary orientations aligned with the transverse orientation. Therefore, more importantly, the results motivate the need to develop modification factors for all orientations so that existing GMMs can be used to estimate spectral accelerations in any specific orientation with respect to the transverse orientation.

To get a better understanding of the influence of epicentral distance on the intensity at the transverse orientation, both $Sa_T/Sa_{RotD100}$ and Sa_T/Sa_{RotD50} were binned by epicentral distance for all stations that recorded the 2022 event. Figure 13 shows the influence of epicentral distance on histograms of the ratio between intensity at the transverse orientation and RotD100 for oscillators with periods of 3, 5, 7, and 10 s. Although there are only 12 records available at epicentral distances less than 30 km, it appears that the intensity at the transverse orientation is more uniformly distributed in this bin. This is consistent with the findings discussed in Figure 8, where it was shown that the orientation of the maximum intensity with respect to the transverse orientation was more uniformly distributed in this distance range. In contrast, at distances greater than 30 km, the distribution of $Sa_T/Sa_{RotD100}$ is clustered towards the right with the intensity at the transverse orientation being, on average, 94% to 97% of RotD100. In general, it is apparent that the intensity at the transverse orientation, on average, gets closer to the RotD100 intensity as epicentral distance increases, although further studies should be conducted using a larger database of ground motions to better estimate this distance dependence. Figure 14 shows the same histograms binned by distance but for the ratio between the intensity at the transverse orientation and RotD50. Similar trends are observed where the intensity at the transverse orientation is, on average, close to the RotD50 intensity in distances less than 30 km, but exceeds RotD50 significantly at longer distances. The implication of this is that RotD50 may not be the best intensity to use in earthquake-resistant design as it has a significant probability of being exceeded and that correction factors to existing RotD50 GMMs should be developed to estimate the level of intensity at specific orientations and that these modification/correction factors may need to account for larger amplification of RotD50 at larger source-to-site distances.

Poulos and Miranda's (2023) main motivation for studying the orientation of the maximum intensity with respect to the transverse orientation was that S-waves from a theoretical strike-slip double couple point source with a vertical dip in a homogenous medium have SH radiation pattern that is more dominant when compared to the SV radiation pattern. Using the epicenter as the source of the radiation patterns, the orientation of the SH waves coincides with the transverse orientation identified above and in the previous section. Therefore, the observations made for this earthquake may be explained by the polarization of S-waves and are therefore primarily the result of a source effect. Site effects such as local geologic heterogeneities, basin edge effects, and topographic irregularities can also cause polarization through filtration of response. Regardless, the orientation of the maximum intensity remains close to the transverse, suggesting the orientation of maximum response is primarily due to source effects.

The discussion above and in the prior section focuses mostly on observations for oscillators with fundamental periods longer than 3 s. While these observations are valuable, it is important to highlight the applicability of the findings for short-period oscillators as well since they typically have large intensities and since most structures tend to have first-mode periods in the short-period range (i.e., 0.1 s to 1 s). From Figures 3, 6, 10, and 11, it is apparent that the observations made for oscillators with periods ≥ 3 s also hold for shorter periods, albeit they are less pronounced. As the oscillator period increases from the short-period range to the long-period range, the intensity at the transverse orientation significantly increases and the orientation of the maximum response gets closer to the transverse orientation. The increased alignment of the orientation of the maximum intensity to the transverse orientation with the increase in oscillator period may be attributed to wave scattering. More specifically, higher frequencies have shorter wavelengths, making them more sensitive to heterogeneities in the Earth's crust.

5. Summary and Conclusions

This work investigated the orientation and intensity of maximum ground motion intensity for 5%-damped linear elastic oscillators subjected to the December 20, 2022 M_w 6.4 Ferndale earthquake. The response of oscillators with periods ranging from 0.1 to 10 s was found to be fairly polarized over the geographic area considered. The orientation of the maximum intensity was found to be, in general, relatively close to the transverse orientation. For example, the fraction of recording stations where the orientation of the maximum response occurred within ±25° of the transverse orientation was found to be, depending on the period of vibration, between 2 (~50%) and 3 (~80%) times the fractions that would occur if the orientation of the maximum response were to be fully random, that is, if all orientations were equally likely to experience the maximum intensity. On average, the orientation of the maximum intensity gets closer to the transverse orientation as the period of the oscillator increases. At epicentral distances less than 30 km, the angular distance between the orientation of the maximum intensity and transverse orientation was found to be more uniformly distributed and without a clear trend for the orientation of the maximum response. At distances greater than 30 km, the orientation of the maximum intensity is close to the transverse orientation. These findings are consistent with the recent study by Poulos and Miranda (2023) for strike-slip earthquakes.

Ground motion intensity at the transverse orientation was found to be, on average, close to the RotD100 intensity for oscillators with periods ranging from 0.1 to 10 s, and these intensities tend to get closer as oscillator period increases. For example, on average, the intensity at the transverse orientation is 91% of RotD100 intensity at 3 s, and this increases to 95% of RotD100 for 10 s. More importantly, it was found that the intensity in the transverse orientation is on average only 10% smaller than the maximum intensity for a wide range of angular differences with respect to the orientation of the maximum intensity (i.e., the intensity at the transverse orientation was at least 90% of RotD100 up to an $|\alpha|$ value of 25°). Additionally, the intensity at the transverse orientation was found to be systematically larger than RotD50, with over 80% of the recording stations experiencing intensities in the transverse orientation that exceeded the RotD50 intensity for periods longer than 4 s. As the oscillator period increases, the average intensity in the transverse orientation is between 1.0 to 1.26 times the RotD50 intensity. The mean Sa_T/Sa_{RotD50} ratios computed in this study could be used as modification/correction factors to RotD50 intensities estimated with existing GMMs in order to estimate the level of intensity at the transverse orientation, which may be a good estimator of maximum intensity. Furthermore, the correction factors to RotD50 were found to have a tendency to increase with increasing source-to-site distance, suggesting that future use of correction factors to estimate intensity at transverse orientation may need to account for larger amplification of RotD50 with an increase in distance. At source-to-site distances less than 30 km, the intensity at the transverse orientation is more uniformly distributed, but at distances greater than 30 km the average intensity at the transverse orientation is 94% to 97% of the RotD100 intensities. Further studies could be carried out to estimate this dependence on source-to-site more precisely using a larger database of ground motions recorded from several strike-slip earthquakes.

Author Statement

Data and Resources

Ground motion records used for the 2022 M_w 6.4 Ferndale earthquake were obtained from the Center for Engineering Strong Motion Data (https://www.strongmotioncenter.org/, last accessed February 2023). The network or agencies providing data in this work are the California Strong Motion Instrumentation Program (CSIMP), the USGS National Strong Motion Project (NSMP), the Berkley Digital Seismograph Network (BDSN), and the UGS Northern California Regional Network (NCSN). Station Code/ID of those used in this work are provided below.

List of CESMD Station Code/ID Used in Study and Corresponding Site Characteristics

Code/ID	Site Class	Code/ID	Site Class	Code/ID	Site Class	Code/ID	Site Class	Code/ID	Site Class
89005	C	1581	N/A	WHMT	N/A	RVIT	N/A	KMPB	N/A
79046	C	1584B	N/A	AONC	N/A	SAGE	N/A	KMR	N/A
79668	C	1023	N/A	BAKR	N/A	TRIN	N/A	KPR	N/A
89255	C	1582	N/A	BJES	N/A	WEAV	N/A	KTD	N/A
89462	D	1586	N/A	BRIC	N/A	KBN	N/A	LASH	N/A
89486	C	1591	N/A	BRIT	N/A	KBU	N/A	LBL	N/A
89641	D	BIGV	N/A	DMOR	N/A	KCO	N/A	LBR	N/A
89688	C	KNEE	N/A	EAGL	N/A	KCR	N/A	LDH	N/A
89781	D	LAB	N/A	GRPK	N/A	KCSB	N/A	LDL	N/A
99640	C	LBE	N/A	HATC	N/A	KCT	N/A	LGY	N/A
99700	C	LBU	N/A	HAYF	N/A	KFP	N/A	LHE	N/A
89734	D	LGMB	N/A	LCOW	N/A	KHBB	N/A	LMC	N/A
89687	D	LWHB	N/A	PETL	N/A	KHMB	N/A	LMI	N/A
1580	N/A	PRDS	N/A	RBOW	N/A	KIP	N/A	LTC	N/A

Acknowledgements

The authors would like to acknowledge the Department of Civil and Environmental Engineering at Stanford University for funding the studies of Nathan Girmay through the Structural Engineering and Geomechanics Fellowship. The authors would also like to acknowledge National Agency for Research and Development (ANID) / Doctorado Becas Chile / 2019-72200307 for funding the doctoral studies of Alan Poulos. The authors are also grateful to the California Strong Motion Program (CSMIP) and the United States Geological Survey (USGS) for installing and maintaining seismic recording stations, and for collecting, processing, and distributing the ground motion records from the 2022 Ferndale earthquake. This investigation would not have been possible without these strong motion records.

References

Abrahamson, N.A., & Silva, W.J. (1997). Empirical response spectral attenuation relations for shallow crustal earthquakes. *Seismological Research Letters*, *68*(1), 94-127.

American Society of Civil Engineers. (2010). Minimum Design Loads for Buildings and Other Structures. *ASCE 7-10 Standard*, American Society of Civil Engineers, Reston, Virginia.

American Society of Civil Engineers. (2016). Minimum Design Loads for Buildings and Other Structures. *ASCE 7-16 Standard*, American Society of Civil Engineers, Reston, Virginia.

American Society of Civil Engineers. (2022). Minimum Design Loads for Buildings and Other Structures. *ASCE 7-22 Standard*, American Society of Civil Engineers, Reston, Virginia.

Ancheta, T.D., Darragh, R.B., Stewart, J.P., Seyhan, E., Silva, W.J., Chiou, B.S.J.,Wooddell K.E., Graves, R.W., Kottke, A.R., Boore, D.M., Kishida, T. & Donahue, J.L. (2014). NGA-West2 database. *Earthquake Spectra*, *30*(3), 989-1005.

Bakun, W.H. (2000). Seismicity of California's North Coast. *Bulletin of the Seismological Society of America* 2000; 90 (4): 797–812.

Beyer, K., & Bommer, J.J. (2006). Relationships between median values and between aleatory variabilities for different definitions of the horizontal component of motion. *Bulletin of the Seismological Society of America*, *96*(4A), 1512-1522.

Boore, D.M., Joyner, W.B., & Fumal, T.E. (1997). Equations for estimating horizontal response spectra and peak acceleration from western North American earthquakes: A summary of recent work. *Seismological Research Letters*, 68(1), 128-153.

Boore, D.M., & Akkar, S. (2003). Effect of causal and acausal filters on elastic and inelastic response spectra. *Earthquake Engineering & Structural Dynamics*, 32(11), 1729-1748.

Boore, D.M. (2004). Choosing the Lowest Usable Frequency for Response Spectra from Filtered Data. Dave's Notes available at www.daveboore.com/daves_notes.

Boore, D.M., Watson-Lamprey, J., & Abrahamson, N.A. (2006). Orientation-independent measures of ground motion. *Bulletin of the Seismological Society of America*, 96(4A), 1502-1511.

Boore, D.M. (2010). Orientation-independent, nongeometric-mean measures of seismic intensity from two horizontal components of motion. *Bulletin of the Seismological Society of America*, *100*(4), 1830-1835.

Boore, D.M., Stewart, J. P., Seyhan, E., & Atkinson, G. M. (2014). NGA-West2 equations for predicting PGA, PGV, and 5% damped PSA for shallow crustal earthquakes. *Earthquake Spectra*, *30*(3), 1057-1085.

Center for Engineering Strong Motion Data (CESMD). Retrieved on January 18, 2023, from https://www.strongmotioncenter.org/index.html

Hong, H.P., & Goda, K. (2007). Orientation-dependent ground-motion measure for seismic-hazard assessment. *Bulletin of the Seismological Society of America*, *97*(5), 1525-1538.

Huang, Y.N., Whittaker, A.S., & Luco, N. (2008). Maximum spectral demands in the near-fault region. *Earthquake Spectra*, 24(1), 319-341.

Joyner, W.B., & Boore, D.M. (1982). Estimation of response-spectral values as functions of magnitude, distance, and site conditions. *Open File Report 82-881*, U.S. Geological Survey.

NEHRP Consultants Joint Venture (2011). Selecting and Scaling Earthquake Ground Motions for Performing Response-History Analysis. *Tech. Rep. NIST GCR 11-917-1*5, National Institute of Standards and Technology, Washington, D.C.

Pacific Earthquake Engineering Research Center (PEER) (2017), Guidelines for Performance-Based Seismic Design of Tall Buildings, Version 2.03, *PEER Report 2017/06*, University of California at Berkeley, Berkeley, California.

Petri, A.E., & Lin, S. (2022, December 21). Northern California towns tally earthquake damage as power is restored to tens of thousands. *Los Angeles Times*. Retrieved March 05, 2023, from https://www.latimes.com/california/story/2022-12-21/california-earthquake-aftermath-damage

Poulos, A., & Miranda, E. (2022a). Proposal of orientation-independent measure of intensity for earthquake-resistant design. *Earthquake Spectra*, 38(1), 235-253.

Poulos, A., Miranda, E., & Baker, J.W. (2022). Evaluation of earthquake response spectra directionality using stochastic simulations. *Bulletin of the Seismological Society of America*, 112(1), 307-315.

Poulos, A., & Miranda, E. (2022b). Probabilistic characterization of the directionality of horizontal earthquake response spectra. *Earthquake Engineering & Structural Dynamics*, *51*(9), 2077-2090.

Poulos, A., & Miranda, E. (2023). Effect of faulting type on the orientation of maximum horizontal earthquake response spectra. *Bulletin of the seismological Society of America*, doi: https://doi-org.stanford.idm.oclc.org/10.1785/0120230001

Shahi, S.K., & Baker, J.W. (2014). NGA-West2 models for ground motion directionality. *Earthquake Spectra*, *30*(3), 1285-1300.

Somerville, P.G., Smith, N.F., Graves, R.W., & Abrahamson, N.A. (1997). Modification of empirical strong ground motion attenuation relations to include the amplitude and duration effects of rupture directivity. *Seismological Research Letters*, *68*(1), 199-222.

Temblor. (2022, December 20). Earthquake rumbles northern California triple junction. Retrieved on March 05, 2023, from https://temblor.net/earthquake-insights/dec-20-2022-ferndale-earthquake-northern-california-14791/

United States Geological Survey (USGS) (2022). M 6.4 - 15km WSW of Ferndale, CA. Retrieved March 5, 2023, from https://earthquake.usgs.gov/earthquakes/eventpage/nc73821036/executive

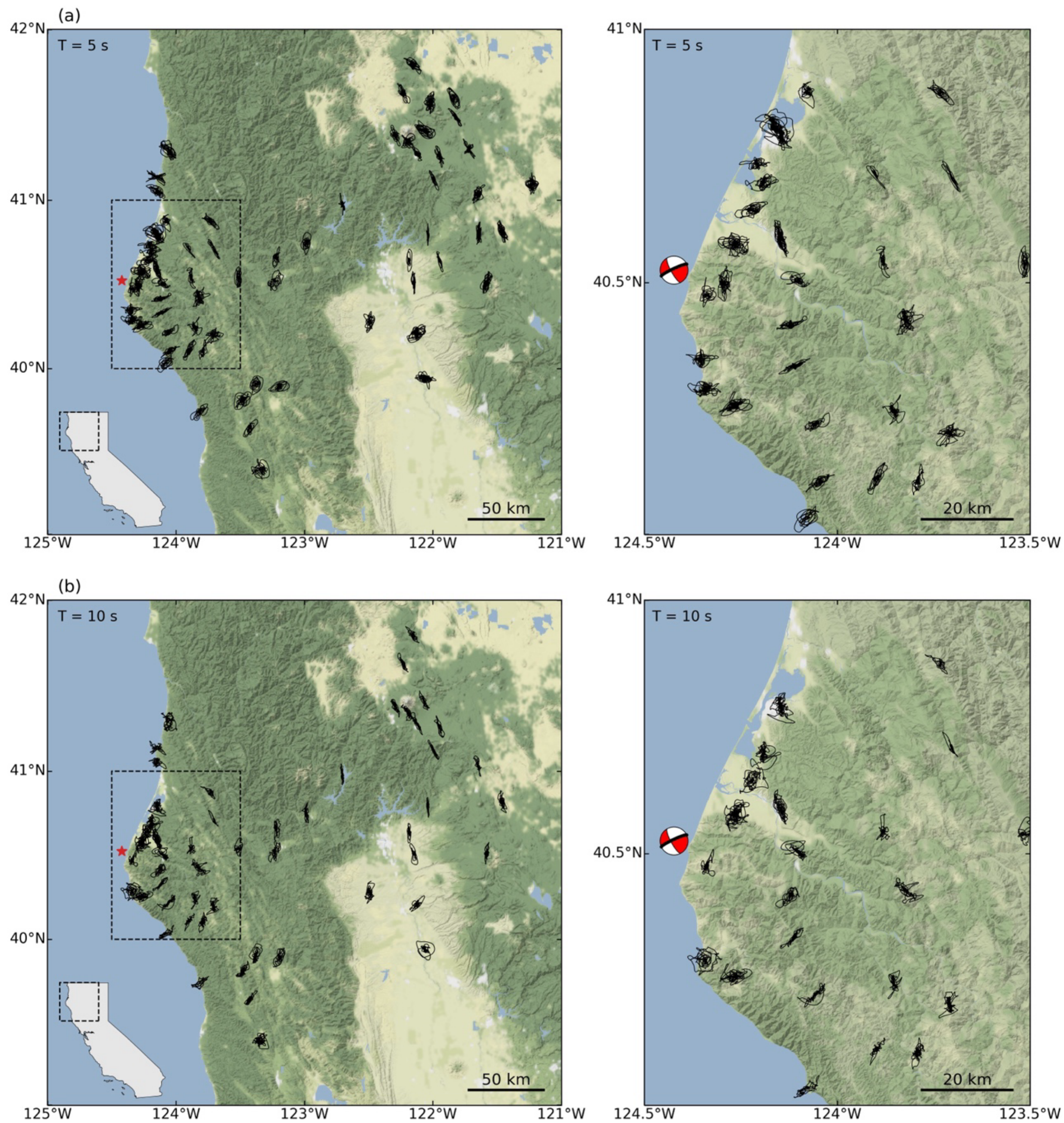

Figure 1: Spatial distribution of relative displacement hodographs of 5% damped linear elastic oscillators subjected to recorded ground motions from the 2022 M_w 6.4 Ferndale earthquake for (a) T = 10 s, and (b) T = 5 s. The epicenter is indicated by the red star and the thicker black line in the focal mechanism indicates the preferred fault plane.

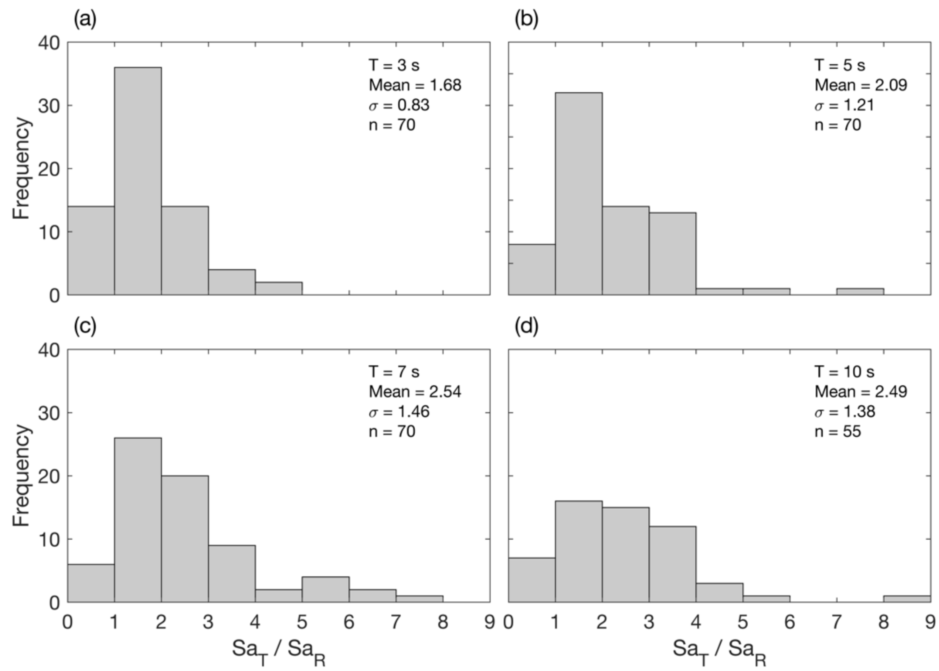

Figure 2: Histograms of the ratio between the ground motion intensity in the transverse orientation to the intensity in the radial orientation for (a) T = 3 s, (b) T = 5 s, (c) T = 7 s, and (d) T = 10 s. Each panel also presents the mean and standard deviation (σ) of the ratio, and the number of records used for each case (n).

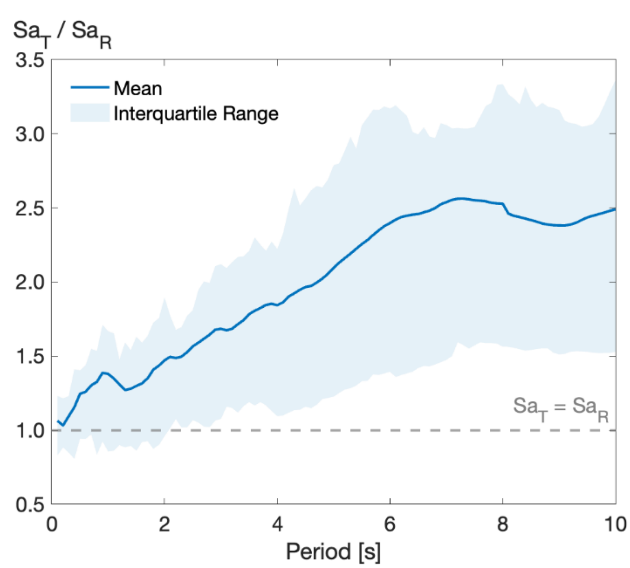

Figure 3: Influence of period of vibration on the level of polarization as measured by the mean ratio between the ground motion intensity in the transverse orientation to the intensity in the radial orientation for periods between 0.1 and 10 s.

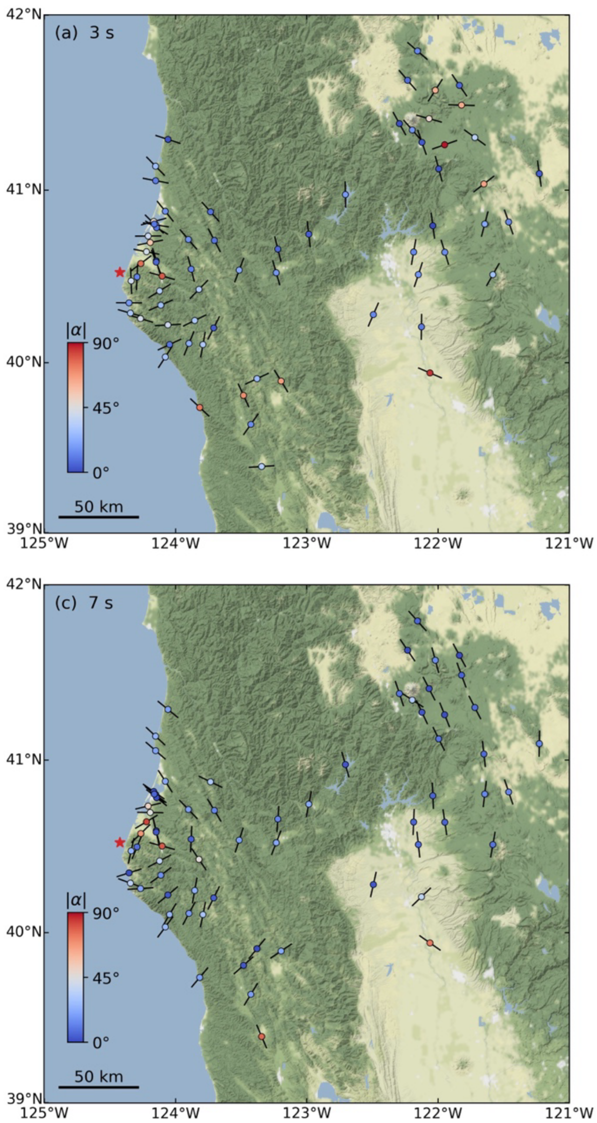

Figure 4: Orientation of the maximum response of 5% damped linear elastic oscillators (indicated by short black lines at each recording station) and their angular distance with respect to the transverse orientation (indicated by the color in each circle) for (a) T = 3 s, (b) T = 5 s, (c) T = 7 s, and (d) T = 10 s.

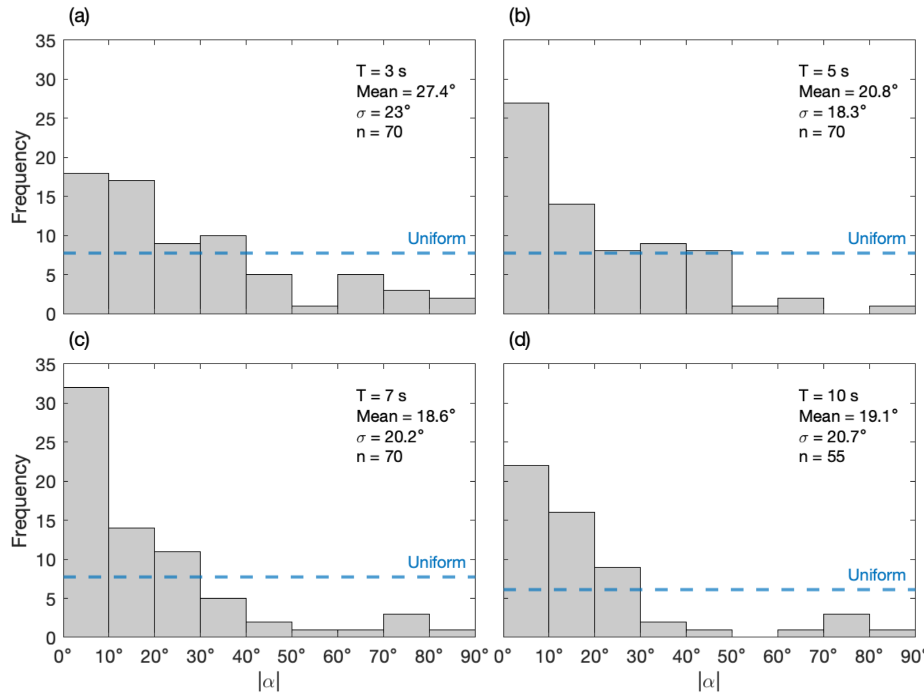

Figure 5: Histogram of angular distance between the orientation of RotD100 and the transverse orientation for oscillators with periods of: (a) T = 3 s, (b) T = 5 s, (c) T = 7 s, and (d) T = 10 s. Dotted line represents the histogram if the orientation of RotD100 were to be equally likely in all orientations. Each panel also presents the mean and standard deviation (σ) of the angles, and the number of records used for each case (n).

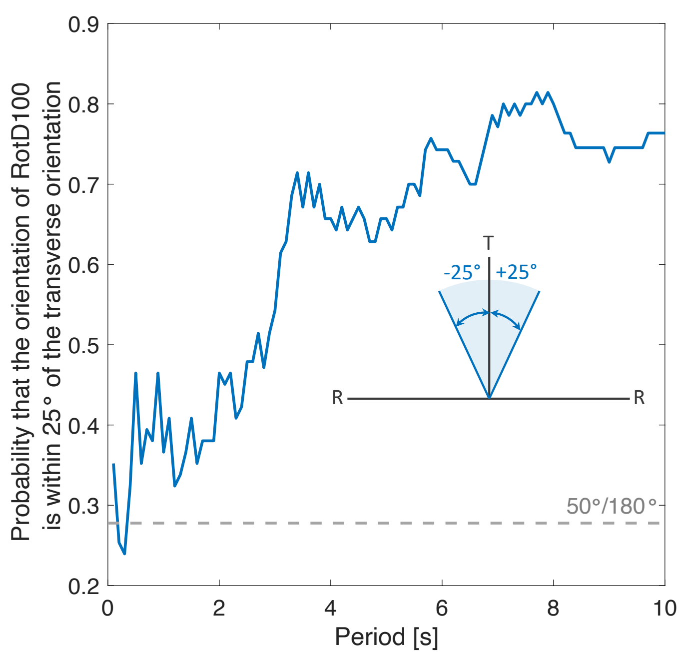

Figure 6: Fraction of stations where the orientation of RotD100 falls within ±25° of the transverse orientation. For a fully random case, the expected fraction would be 50°/180° (0.28).

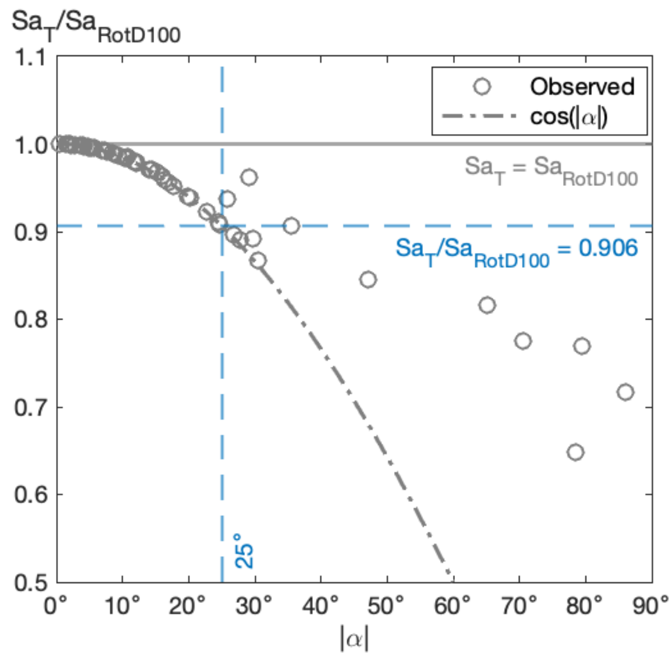

Figure 7: Relationship between $|\alpha|$ and the ratio of the intensity at the transverse orientation to the maximum intensity at each recorded station for a period of 10 s.

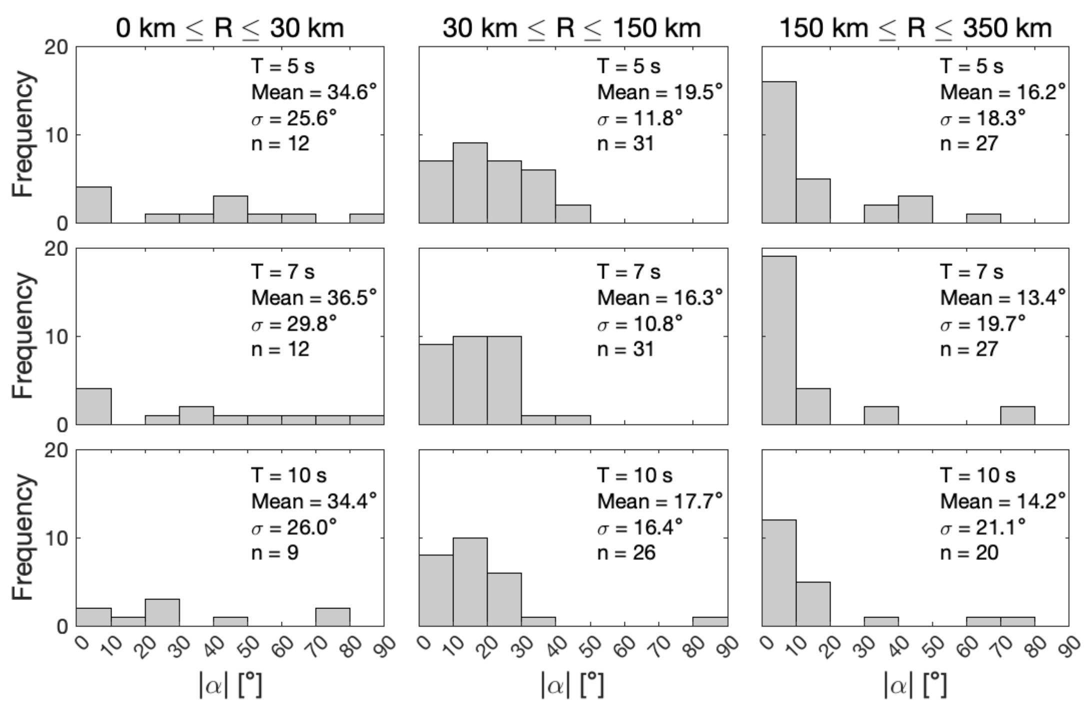

Figure 8: Influence of epicentral distance (R) on the histograms of angular difference between the orientation of RotD100 and the transverse orientation for oscillators with periods of 5, 7, and 10 s. Each panel presents the mean and standard deviation (σ) of the angles, and the number of records used for each case (n).

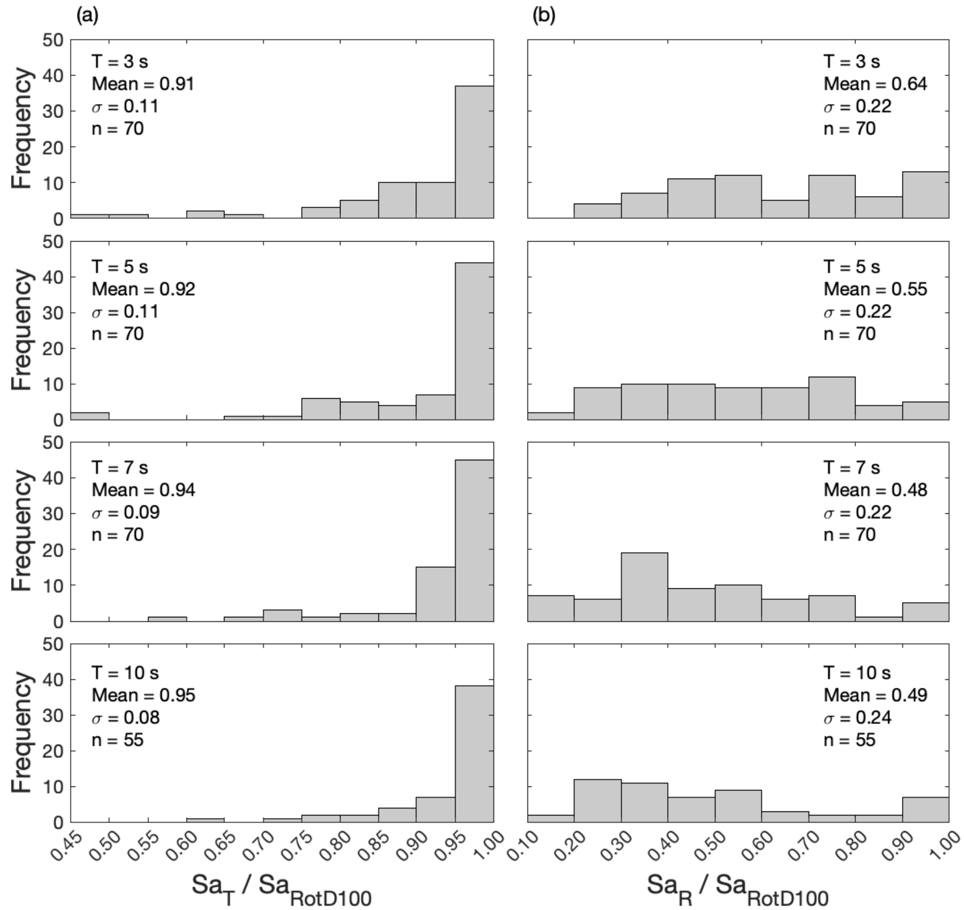

Figure 9: Histogram of the ratio between the ground motion intensity at the (a) transverse or (b) radial orientation and RotD100 for periods of 3, 5, 7, and 10 s. Each panel presents the mean and standard deviation (σ) of the ratios, and the number of records used for each case (n).

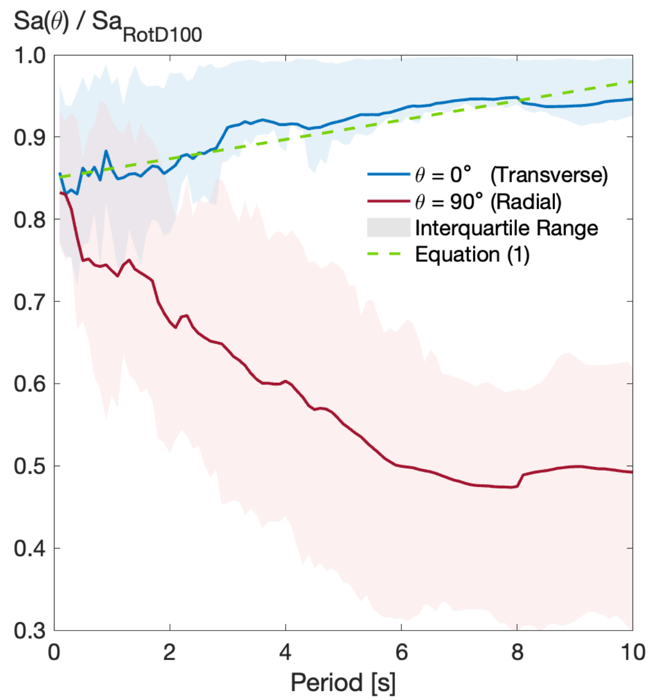

Figure 10: Mean ratio between the ground motion intensity at the transverse orientation and the RotD100 intensity and between the intensity at the radial orientation and the RotD100 intensity for periods between 0.1 and 10 s. Shaded bands around means show the interquartile ranges at each period.

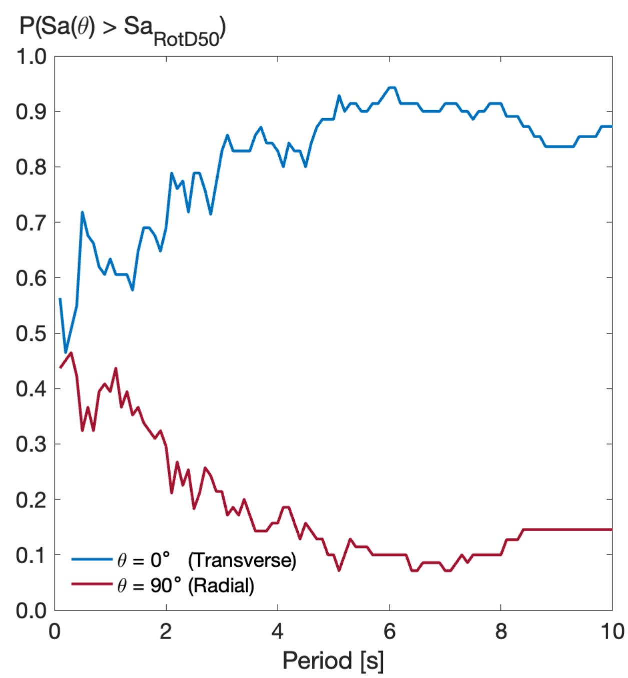

Figure 11: Fraction of stations where the intensity at the transverse or radial orientation exceeds the RotD50 intensity.

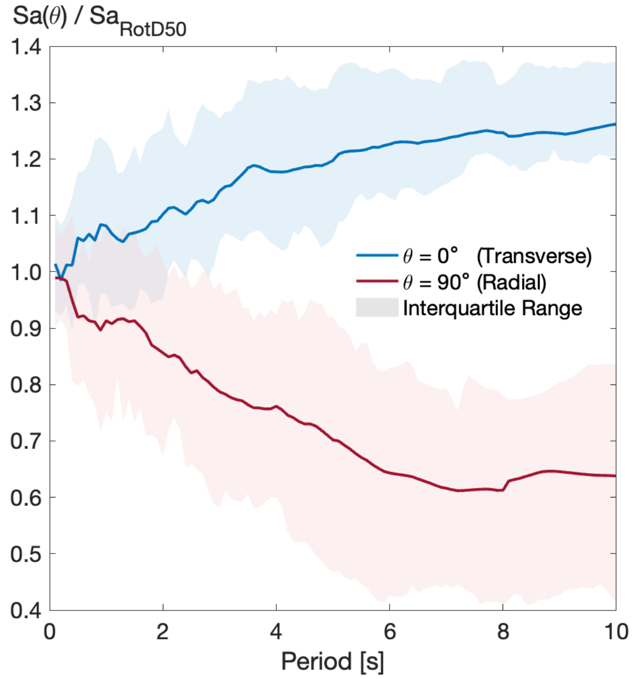

Figure 12: Mean ratio between the ground motion intensity at the transverse orientation and the RotD50 intensity and between the intensity at the radial orientation and the RotD50 intensity for periods between 0.1 and 10 s. Shaded bands around means show the interquartile ranges at each period.

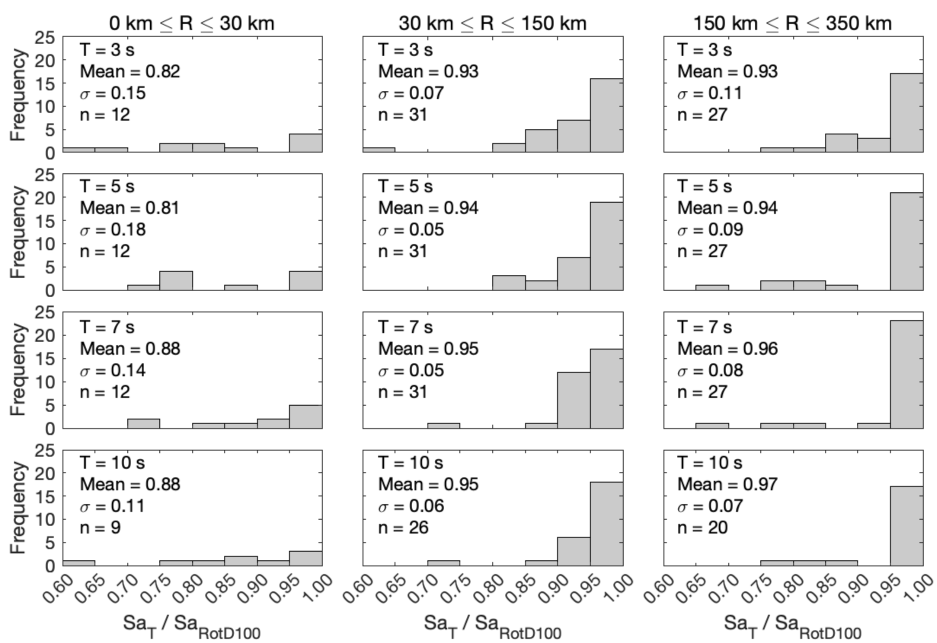

Figure 13: Influence of epicentral distance (R) on histograms of the ratio between the ground motion intensity at the transverse orientation and RotD100 for oscillators with periods of 3, 5, 7, and 10 s. Each panel presents the mean and standard deviation (σ) of the ratios, and the number of records used for each case (n).

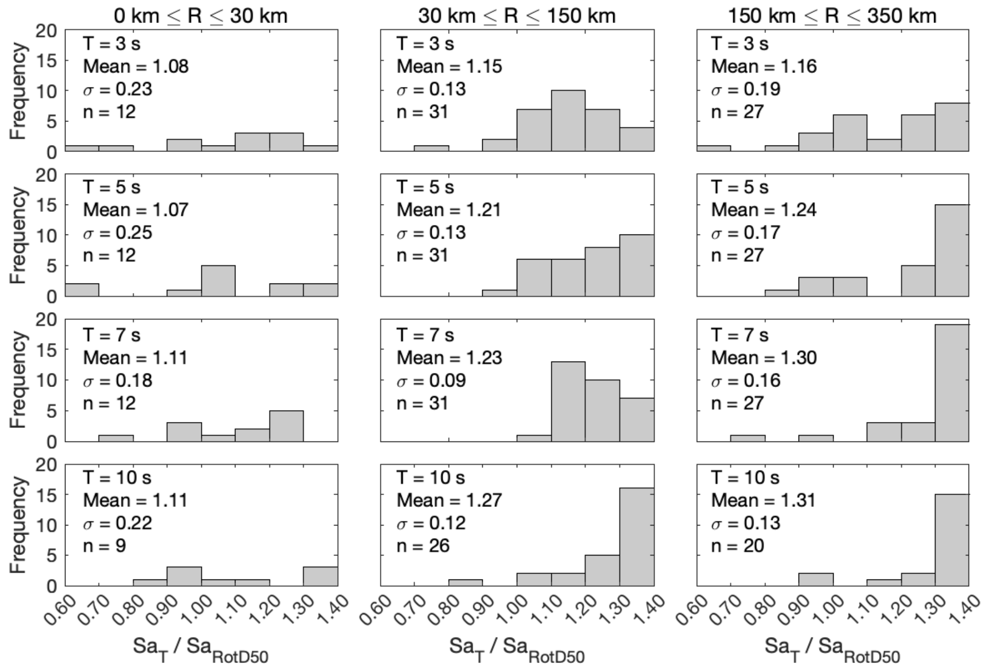

Figure 14: Influence of epicentral distance (R) on histograms of the ratio between the ground motion intensity at the transverse orientation and RotD50 for oscillators with periods of 3, 5, 7, and 10 s. Each panel presents the mean and standard deviation (σ) of the ratios, and the number of records used for each case (n).